Organic & Biomolecular Chemistry

Dynamic Article Links

Cite this: *Org. Biomol. Chem.*, 2011, **9**, 8006

www.rsc.org/obc

PAPER

Tuning the activity of glutathione peroxidase mimics through intramolecular Se · · · N,O interactions: A DFT study incorporating solvent-assisted proton exchange (SAPE)†

Craig A. Bayse* and Andrea Pavlou

Received 25th May 2011, Accepted 30th August 2011
DOI: 10.1039/c1ob05827d

Diaryl diselenide mimics of the antioxidant selenoprotein glutathione peroxidase (GPx) often incorporate intramolecular Se · · · N,O interactions to enhance their GPx-like activity. Although the strength of the interaction is defined by the Lewis basicity of the donating group and the strength of the Se–X bond, there is not a clear relationship between the interaction and the GPx-like activity. Density-functional theory and natural bond orbital (NBO) calculations are used to show the range of Se · · · N,O interactions for various functional groups. The strongest interactions are found for groups which stabilize the donor–acceptor interaction through aromatic stabilization. The activation barriers for the GPx-like mechanism of activity of several substituted areneselenols are calculated using DFT and solvent-assisted proton exchange (SAPE), a technique that incorporates networks of solvent molecules into the theoretical model to facilitate proton transfer between sites in the reactant and product. DFT-SAPE models show that, in addition to decreasing the barrier to oxidation of the selenol, Se · · · N,O interactions generally increase the barriers for selenenic acid reduction and selenol regeneration because the Se · · · N,O interaction must be broken for the reaction to proceed. Calculated activation barriers for the rate-determining step are consistent with the relative experimental GPx-like activities of a series of diaryl diselenides.

Introduction

Small molecule mimics of the selenoenzyme glutathione peroxidase (GPx) are of interest for their potential application to the prevention of diseases related to oxidative stress.[1–4] The ability of these organoselenium compounds to scavenge reactive oxygen and nitrogen species (ROS/RNS) is often influenced by covalent and non-covalent interactions of selenium with nitrogen and oxygen groups.[1,2,5] Ebselen **1** and other selenenamides incorporate a direct Se–N bond and have been widely studied as GPx mimics.[6] Ebselen is nontoxic, unlike many selenium compounds, and has been used in clinical trials for the prevention of acute oxidative stress during stroke.[7] Highly-active GPx mimics with direct Se–O bonds – cyclic seleninates (*e.g.*, **2**) and selenuranes (*e.g.*, **3**) – have been synthesized by Back and others.[8–12] Se–N covalent bonding has also been shown for the oxidation products of selenomethionine (SeMet).[13]

A number of diselenide GPx mimics incorporating intramolecular non-bonding Se · · · N interactions have been synthesized based upon observations of the enzyme active site in which tryptophan and glutamine are found with selenocysteine (SeCys) and conserved throughout the GPx family.[14] These compounds were originally aromatic diselenides with an amine or amide group *ortho* to the selenium center (*e.g.*, **4a** [Note: For **4–15**, if X is not designated, the compound is the homo-diselenide.]. Wirth later showed that GPx-like activity could also be enhanced by *ortho*-substitution of oxygen donors.[15] Non-bonding Se · · · N interactions have also been incorporated into selenenium-based cationic GPx mimics.[16] However, it is not clear how these interactions affect the reactivity of Se in substituted diselenides. The Se · · · N interaction was proposed to tune reactivity at the selenium center of the molecule,[14] but more recently, Mugesh has shown that strong Se · · · N,O interactions favor simple thiolate substitution in selenenyl sulfide intermediates, which reduces GPx-like activity.[17] In addition to modifying GPx-like activity, these interactions have also been used to stabilize highly reactive Se(II) functionalities such as selenenyl azides.[18]

$$\mathrm{ROOH + 2RSH \rightarrow ROH + RSSR} \quad (1)$$

Mimics of GPx catalyze the same overall reaction (eqn (1)) as the enzyme, but often through different, more complex pathways.[1,19] Diselenides are likely to follow a mechanism similar to the

Department of Chemistry and Biochemistry, Old Dominion University, Hampton Boulevard, Norfolk, Virginia, USA. E-mail: cbayse@odu.edu; Fax: 01 757 683 4628; Tel: 01 757 683 4097

† Electronic supplementary information (ESI) available. See DOI: 10.1039/c1ob05827d

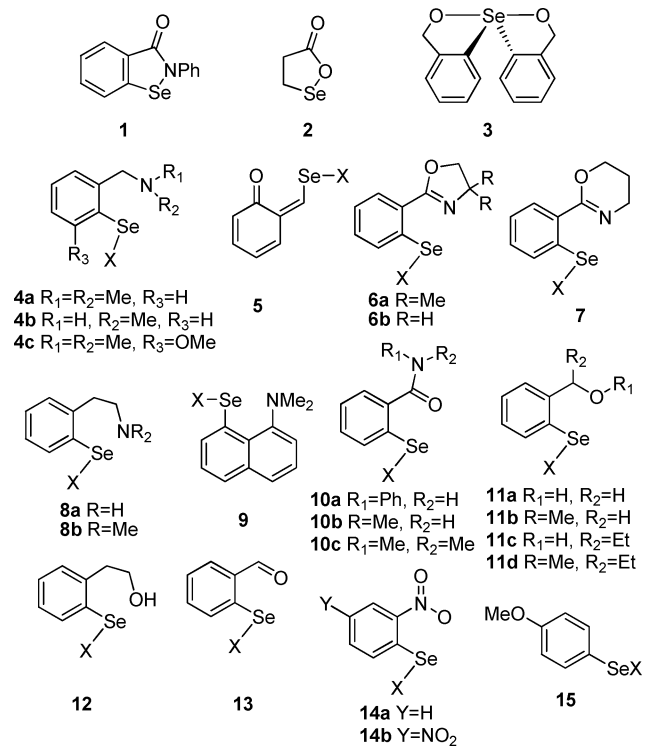

three-step enzymatic cycle of GPx (Scheme 1)[20] – (1) oxidation of the selenol *E*-SeH to the selenenic acid *E*-SeOH, (2) reduction of *E*-SeOH to *E*-SeSG by attack of glutathione (GSH) and (3) regeneration of *E*-SeH by thiol reduction – because the Se–Se bond is first cleaved by an equivalent of thiol to form one equivalent each of selenol and selenenyl sulfide. In biological systems, RSH may be any available thiol, including the cysteinates of zinc-finger transcription factors. In fact, reducible selenium compounds such as ebselen have been shown to release zinc from transcription factors which may disrupt transcription and DNA repair, possibly impacting genomic integrity.[21,22]

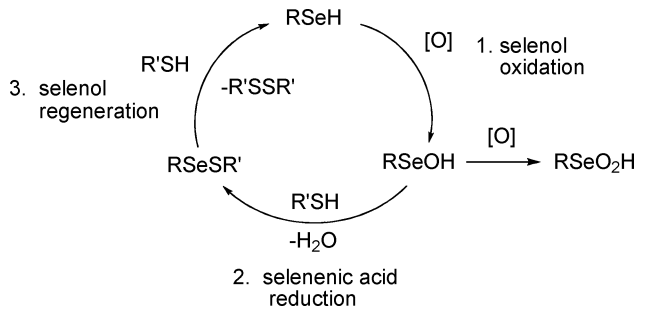

Scheme 1 Mechanism for catalytic scavenging of ROS by GPx and other selenols.

$$\mathrm{RSe}\mathit{H} + \mathrm{R'OOH} \rightarrow \mathrm{RSeOH} + \mathrm{R'O}\mathit{H} \qquad (2)$$

Molecular modeling is an important tool for understanding the speciation and biological activity of selenium compounds.[23] However, theoretical exploration of the GPx-like mechanism of these species is complicated by proton exchange in the individual mechanistic steps. For example, in the first step of the GPx-like cycle (eqn (2)) the selenol proton (italicized) must be transferred to the emerging alcohol. This is not a direct transfer between the selenium and oxygen centers, but an indirect process facilitated, and effectively catalyzed, by the surrounding bulk water. Because proton exchange is an inherently solution-phase process, realistic modeling of these mechanistic steps is a challenge to gas-phase *ab initio* and DFT methods. Early computational studies of the GPx mechanism using direct proton transfer result in high-energy transition states that would be unlikely in solution phase.[24–27] Our group and others have incorporated small water clusters into computational models in order to account for the participation of bulk solvent in reactions involving proton exchange.[28–34] We refer to this technique of microsolvation as solvent-assisted proton exchange (SAPE) in order to distinguish it from other methods of explicit solvation. SAPE has been used to examine the mechanisms of the oxidation of ebselen and other organoselenium compounds[28] and the reduction of seleninic acids.[29] SAPE models of the GPx-like cycle for benzeneselenol (PhSeH) produced activation barriers[30] consistent with experimental observations of the enzyme and previous DFT studies of the truncated active site.[35] In the following paper, we extend this study of PhSeH to examine the effect of Se···N,O interactions on the GPx-like mechanisms of aromatic selenols.

Theoretical methods

SAPE models incorporate a network of protic solvent molecules to approximate the solution-phase acid/base chemistry that facilitates proton exchange. The solvent molecules connect the sites of protonation in the reactants and products such that a proton is shuttled through the hydrogen-bonding network concurrent with heavy atom bond breaking/forming. The SAPE network is intended to mimic (in a first approximation) the role of solvent in a process involving proton exchange rather than to reproduce solvation of the chemical system. The reactant complexes are local minima subject to the constraint that the hydrogen bonding network remains intact and are not necessarily the absolute global minimum for the reactant-water cluster. Based upon comparisons between various DFT exchange–correlation (xc) functionals and post-Hartree–Fock *ab initio* methods (MP2 and CCSD/MP2) for the oxidation of MeSeH by MeOOH using a two-water SAPE network, the mPW1PW91 xc functional provides the best agreement with the higher level *ab initio* results ($\Delta\Delta G^{\ddagger}$ = 2 kcal mol^{-1}).[23] The admixture of Hartree–Fock exchange appears to be important as pure DFT functionals and hybrid functionals with high percentages of HF exchange significantly under- and overestimate, respectively, activation barriers.

Geometry optimizations were performed at the DFT/mPW1PW91[38] level in Gaussian 03.[39] For basis set I (BSI), selenium was represented by the Hurley *et al.* relativistic effective core potential (RECP) double-ζ basis set[40] augmented with a set of even-tempered s, p, and d diffuse functions. The Wadt–Hay ECP basis set modified with diffuse s- and p-functions was used for sulfur and halogen centers.[41] Nitrogen, oxygen and hydrogens not bonded to carbon were represented by Dunning's split-valence triple-ζ plus polarization function basis set (TZVP).[42] Basis sets for hydrocarbon fragments were double-ζ quality.[43] For the SAPE models, geometries were calculated using a larger basis set (BSII) in which an additional set of diffuse and polarization functions on were included in the basis sets for Se, S, O, N and C (polarization only). Basis sets for hydrogens attached to non-carbon heavy atoms were TZVP quality. Bulk solvation effects in water were calculated with the PCM model[44] using Bondi radii[45] for all atoms.

Results and discussion

Strengths of Se···N,O interactions. Barton *et al.*[46] described the Se···O intramolecular interactions in **4-Me** and **4-Cl** in terms of valence bond theory as related to a three-center-four-electron bond. Donation of a lone-pair from the Lewis base partially expands the octet of the selenium center for a linear L–Se–X interaction analogous to a T-shaped hypervalent molecule. The resonance structures (eqn (3)) for this interaction emphasize the relationship between the strength of the interaction and the strength of the Lewis base donor. Strong donors increase the admixture of the right-hand resonance structure to increase the hypervalency of the selenium center. An important consequence of the Se···N,O interaction demonstrated by Mugesh[17] is that strong donors are poor GPx mimics. Donation of electron density to the selenenyl sulfide intermediate increases the partial negative charge of the sulfur center. This decrease in electrophilicity reduces the rate of selenol regeneration *via* step 3 and favors catalytically unproductive thiol exchange.

$$L:Se\text{–}X \leftrightarrow L\text{–}Se^{+}\ X^{-} \qquad (3)$$

Shifting to a molecular orbital theory picture, the strength of the bonding MO is also important because the lone-pair acceptor is the Se–X antibonding MO.[47] The more stable the Se–X bonding MO, the higher in energy the antibonding MO such that overlap with the donating lone pair MO is less favorable. The strength of donor–acceptor interactions may be estimated using Natural Bond Orbital (NBO) theory through a perturbative treatment of the localized MOs.[48] Tomoda *et al.* have used NBO analysis in several studies to measure the strength of the interaction between selenium and nitrogen,[49–51] oxygen,[52,53] and the halides.[54,55] NBO calculations by Mugesh have been used to understand the reactivity of various GPx mimics[17,56] and our group has shown that the strength of the Se···N,O interaction depends upon the functionality of the donating atom.[47] For example, amines are stronger donors than alcohols but, the resonance structures of an amide make the carbonyl oxygen a better donor than the amide NR_2 group. We concluded that, although the NH_2 of Gln faces Se in the crystal structure of GPx-SeO_2H due to hydrogen bonding with the seleninic acid, Se···O interactions with the carbonyl should have more effect on the reactivity of the selenium functional groups within the GPx cycle. However, Morokuma's DFT study of the GPx active site found similar activation barriers for models in which Se interacts with either group.[35] Our group has also investigated these interactions in selenoxide elimination from *Se*-substituted selenocysteines,[57] and [2,3]-sigmatropic rearrangements of allylic selenoxides.[58]

Before examining the effect of Se···N,O interactions upon the GPx-like mechanism in Scheme 1, we briefly discuss the strengths of these interactions for a series of 84 *ortho*-substituted divalent arylselenium compounds (**4–15** where X = Me, SMe, SeMe, CN, SCN, N_3, Cl, Br, I and OH). Geometries of these species (see Tables S1–S4 in ESI†) were optimized at the DFT(mPW1PW91)/BSI level followed by NBO calculations of the donor–acceptor energy ($\Delta E_{d\rightarrow a}$). These structures are consistent with the results of various prior theoretical studies.[46,49–53,56]

The plot of $\Delta E_{d\rightarrow a}$ *versus* the Se···N,O distance in Fig. 1 is consistent with expectations from the VB and MO models. The donor–acceptor energy is inversely proportional to the Se···N,O distance and asymptotically approaches zero as the Se···N,O distance increases. Short Se···N,O distances correlate with strong donation of electron density from the donor group and are found for those systems with strong Lewis base donors and weak Se–X bonds (see Table S1 in ESI†). The highly covalent Se–C bonds of the selenides (X = Me) correspond to the lowest $\Delta E_{d\rightarrow a}$ values and the longest Se···N,O distances (*i.e.*, **6b-Me** 2.80 Å and 4.6 kcal mol^{-1}) whereas the highly polar selenium-halogen bonds appear at short Se···N,O distances and high donor–acceptor energies (*i.e.*, **6b-Cl**: 2.18 Å and 64.2 kcal mol^{-1}; see Fig. 2). The

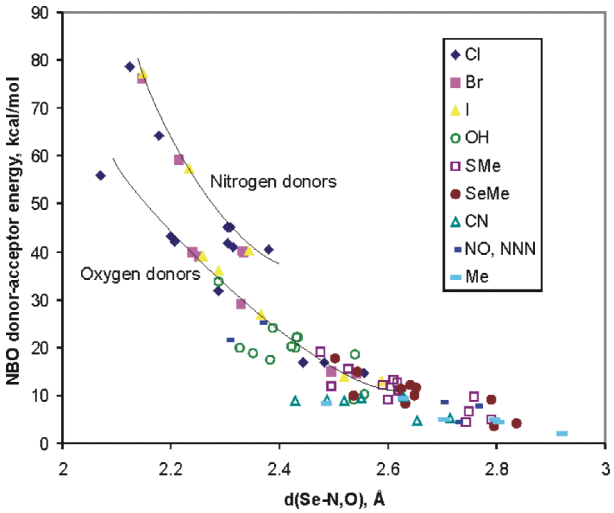

Fig. 1 Correlation between the Se···N,O distance and the NBO donor–acceptor energy for **4–15-X** (See ESI† for additional details). Lines indicate the trends for nitrogen and oxygen donors for the selenenyl halides only.

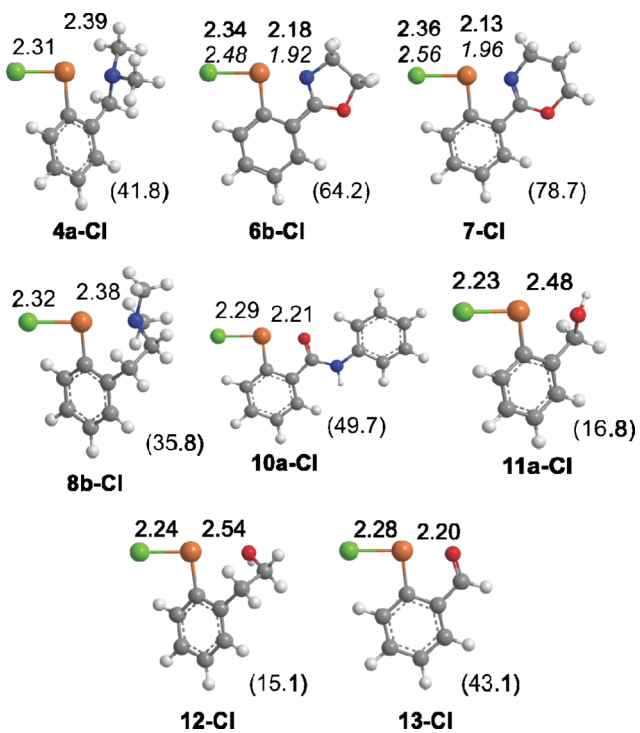

Fig. 2 Se···N,O distance and the NBO donor–acceptor energy for selected selenenyl chlorides. Experimental values are italicized.[36,37]

strong interactions of the selenenyl halides allow a broader range of interaction energies, such that the relative Lewis basicity of nitrogen- and oxygen-containing groups is distinguishable (Fig. 1). For example, the basic amine of **4a-Cl** interacts more strongly than the analogous ether **11b-Cl** ($\Delta E_{d\rightarrow a}$ = 41.8 *vs.* 16.9 kcal mol^{-1}; d(Se–Cl): 2.321 *vs.* 2.237 A). Extending the length of the donor's tether decreases the strength of the interaction. Comparing the alcohols **11a-Cl** and **12-Cl** and amines **4a-Cl** and **8b-Cl**, there is a slight decrease in $\Delta E_{d\rightarrow a}$ due to the steric requirements of formation of the six-membered ring by the Se···N,O interaction. The GPx-like activity of diselenide **12** is half that of **11a**,[15] perhaps attributed to a weaker Se···O interaction. Bulky R groups also reduce the donor–acceptor interactions for the series *ortho*-substituted benzyl amine selenenyl sulfides (**4a-SMe** > **4d-SMe** ($R_{1,2}$ = Et) > **4e-SMe** ($R_{1,2}$ = iPr); see Table S3†) which may contribute to the overall reduction in the GPx-like activity of the series of analogous homo diselenides.[59]

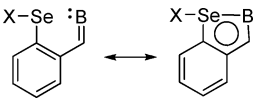

(4)

Se···N,O interactions are enhanced by aromatic stabilization if the donor atom is unsaturated, in conjugation with the aromatic ring and the number of π-electrons fulfills the Hückel rule (eqn (4)).[60,61] The effect of aromatic stabilization can be shown by comparing **11a-Cl** and **13-Cl** to the analogous simple donor–acceptor complexes MeSeCl·L (L = H_2O, HCHO) where water forms a stronger interaction than formaldehyde ($\Delta E_{d\rightarrow a}$ = 8.8 *vs.* 5.0 kcal mol^{-1}). In contrast, the aldehyde group of **13-Cl** forms a very strong Se···O interaction, double that of benzyl alcohol **11a-Cl** ($\Delta E_{d\rightarrow a}$ = 16.8 *vs.* 43.1 kcal mol^{-1}), because the five-membered ring formed by the Se···O interaction has the correct number of electrons for an aromatic π system. Similar interactions are observed in the X-ray structures of **6a-X**[36] and **7-X**[37] and our DFT calculations of **6b-X** and **7-X** (X = Cl, Br, I) where the nitrogen donor atoms form very strong Se···N,O interactions ($\Delta E_{d\rightarrow a}$ = 64.2 (**6b-Cl**); 78.7 (**7-Cl**)). The $\Delta E_{d\rightarrow a}$ value for **7-Cl** is stronger than **6b-Cl** because the bond angles of the six-membered oxazyl ring of **7-Cl** lead to more favorable bond angles for ring formation by the Se···N interaction. The chloride **7-Cl** has the shortest Se···N and the longest Se–X distances (2.125 and 2.364, respectively) of any molecule included in this study with the notable exception of **5** which is a unique example of a Se···O interaction.[46] Aromatic stabilization of the Se···O interaction in **10a-SMe** may explain the low activity of ebselen and amide-based GPx diselenides as the NBO interaction energy $\Delta E_{d\rightarrow a}$ in **10a-SMe** (11.8 kcal mol^{-1}) is slighter greater than that for **6b-SMe** (10.9 kcal mol^{-1}), a derivative of an inactive diselenide. Mugesh has shown that *tert*-amides such as **10c** have higher activity than the related *sec*-amides.[62] This improved activity may be attributed to steric interactions between the R-groups and the ring in **10c** which prevent the *tert*-amide from adopting the planar configuration found for **10b** such that the Se···O distance is significantly longer (2.714 *vs.* 2.479 Å) and $\Delta E_{d\rightarrow a}$ is lower than the *sec*-amide (5.0 *vs.* 18.4 kcal mol^{-1}).[62]

Effects of Se···N,O interactions on the reaction pathway. To determine the effect of Se···N,O interactions upon the GPx-like cycle of aryl selenols, transition states were determined for the three steps of the GPx cycle (Scheme 1) for four model compounds using SAPE networks similar to our previous work on PhSeH.[30] Compounds selected for this study include three *ortho*-substituted selenols with Lewis base donors of varying strength: **11a** (OH, weak), **4a** (NMe_2, strong), and **14a** (NO_2, strong due to aromatic stabilization).

Table 1 DFT(mPW1PW91)/BSII activation parameters and reaction energies (ΔH and ΔG)[a] for step 1 of the GPx-like mechanism of selenols (selenol oxidation)

	$\Delta H^{\ddagger}$	$\Delta G^{\ddagger}$	$\Delta G^{\ddagger}+\Delta G_{solv}$[c]	ΔH_{rxn}	ΔG_{rxn}
Ph[b]	12.7	19.4	19.1	−59.1	−57.2
4a	13.4	23.2	16.0	−68.5	−62.9
11a	12.2	22.5	15.2	−62.7	−59.6
14a	13.8	25.1	17.7	−63.3	−61.2
15	13.2	21.5	17.1	−58.9	−57.0

[a] All energies are calculated relative to the reactant complex **R1**. [b] Reference 30. [c] PCM correction for solvation in water.

For comparison, the reaction pathway for *p*-methoxybenzeneselenol **15-H** was also calculated as a contrast to the trends shown for Se···N,O interactions. In the following discussion, reported energetics are the solvation-corrected Gibbs free energies ($\Delta G+\Delta G_{solv}$). Activation parameters and reaction energies are given in Tables 1–3 and selected bond distances are shown in Fig. 3–5 for each stationary point of **4a** and the transition states only all other species. Stationary points in the following discussion are designated by the fragment number and the position on the reaction pathway (*e.g.*, **15-TS2** is the step 2 transition state complex for fragment **15**).

Step 1: *Selenol oxidation*. The reactant complex **R1** (Scheme 2) for oxidation of selenol by MeOOH incorporates a SAPE network of two water molecules to form a hydrogen bonding network from the selenol to the methoxy oxygen. From this initial complex, heterolytic cleavage of the O_A–O_B bond to transfer O_AH^+ to the selenium center increases the negative charge at O_B to drive proton transfer from the selenol, ultimately forming MeOH and ArSeOH. MeOOH approaches the selenium center perpendicular to the plane of the Se···N,O interaction and the pendant group does not appear to have a steric effect on the oxidation (e.g, **4a-R1** in Fig. 3). For the oxidation of PhSeH, the activation barrier (19.1 kcal mol^{-1})[30] using the same SAPE network was similar to the experimental value for GPx (14.9 kcal mol^{-1}) and the stepwise barrier for a DFT model of the GPx active site (17.1 kcal mol^{-1}).[35]

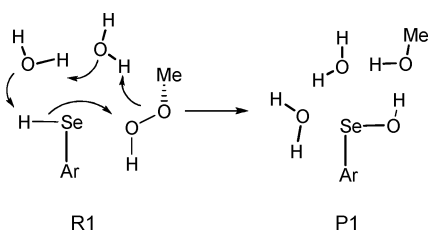

Scheme 2 SAPE network for step 1 of the GPx-like mechanism.

The transition states **4a-TS1**, **11a-TS1**, and **14a-TS1**(Fig. 3) show that transfer of the OH group occurs at longer O–O and shorter Se–O distances (1.94 and 2.13 Å, respectively for **11a-TS1**) than for oxidation of the parent PhSeH (1.88 and 2.20 Å, respectively)[15] due to the decrease in nucleophilicity of the selenol induced by the Se···N,O interaction. This shift to late transition

Table 2 DFT(mPW1PW91)/BSII activation parameters and reaction energies (ΔH and ΔG)[a] for step 2 of the GPx-like mechanism of selenols (selenenic acid reduction)

	ΔH_{int}	ΔH_{int}	$\Delta G_{int} + \Delta G_{solv}$[c]	$\Delta H^{\ddagger}$	$\Delta H^{\ddagger}$	$\Delta G^{\ddagger} + \Delta G_{solv}$[c]	ΔH_{rxn}	ΔG_{rxn}	$\Delta E_{d \to a}$ (X = OH)
Ph[b]	—	—	—	2.5	4.9	6.6	−24.0	−26.3	—
4a	3.3	8.8	5.2	9.0	16.2	15.2	−19.3	−17.8	20.0
11a	1.5	4.7	9.3	0.4	6.4	10.5	−26.5	−27.1	10.4
14a	12.0	15.0	14.9	13.5	19.5	19.7	−17.7	−14.8	17.4
15	—	—	—	1.6	4.2	4.7	−23.4	−24.3	—

[a] All energies are calculated relative to the reactant complex **R2**. [b] Reference 30. [c] PCM correction for solvation in water.

Table 3 DFT(mPW1PW91)/BSII activation parameters and reaction energies (ΔH and ΔG)[a] for step 3 of the GPx-like mechanism of selenols (selenol regeneration)

	ΔH_{int}	ΔG_{int}	$\Delta G_{int} + \Delta G_{solv}$[c]	$\Delta H^{\ddagger}$	$\Delta G^{\ddagger}$	$\Delta G^{\ddagger} + \Delta G_{solv}$[c]	ΔH_{rxn}	ΔG_{rxn}	$\Delta E_{d \to a}$ (X = SMe)
Ph[b]	—	—	—	16.4	23.2	21.7	4.4	4.8	—
4a	9.6	11.4	9.3	19.8	28.4	27.2	6.7	11.3	12.3
4b	2.6	4.9	7.2	14.4	22.6	25.4	8.0	8.3	13.3
4c	5.5	5.4	1.9	20.7	24.9	21.2	2.3	−1.5	6.8
11a	−4.1	0.2	4.5	16.6	20.7	22.5	1.8	3.2	5.0
14a	9.0	9.9	11.3	19.7	26.7	26.1	3.4	5.1	14.0
15	—	—	—	17.2	23.5	21.3	5.8	5.9	—

[a] All energies are calculated relative to the reactant complex **R3**. [b] Reference 30. [c] PCM correction for solvation in water.

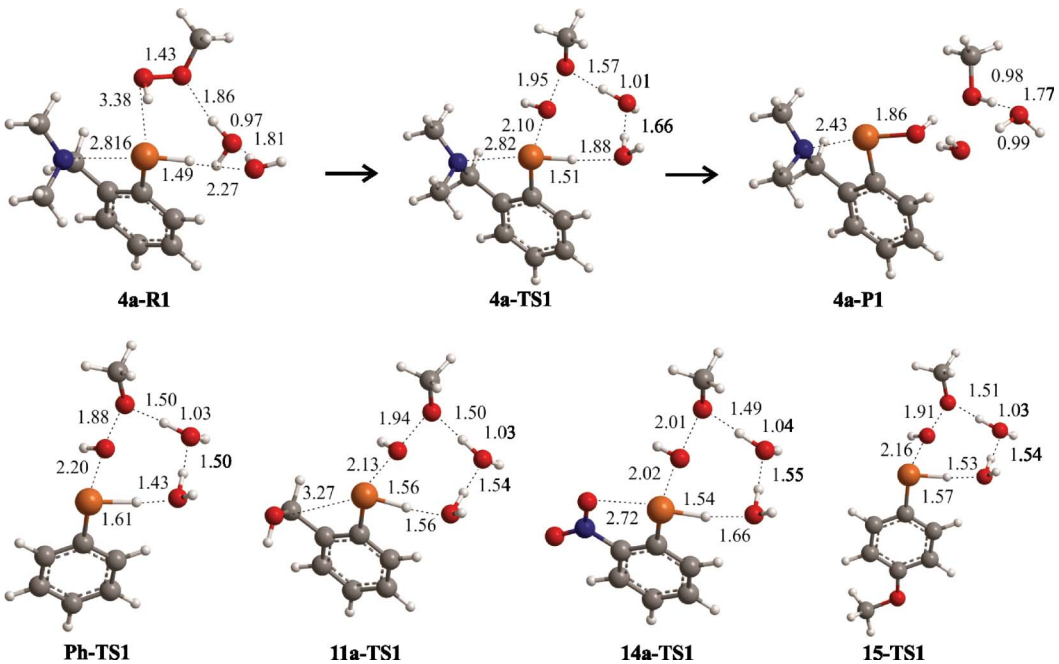

Fig. 3 Selected bond distances for step 1 of the GPx-like mechanism of selenols (selenol oxidation). All stationary points are shown for MeOOH oxidation of **4a-H**; TS1 structures are provided for PhSeH,[30] **11a-H**, **14a-H** and **15-H**. All distances are in Ångstroms.

states relative to PhSeH is consistent with the strength of the Se···N,O interaction ($\Delta E_{d \to a}$ trend: NO_2 > NMe_2 > OH) and the higher (uncorrected) activation barriers (Table 1). Because donation into the Se–H antibonding MO is relatively weak, the effect of Se···N,O interactions on the activation barrier is small, less than 2–6 kcal mol^{-1} higher than for PhSeH. Correction for solvation reduces the barriers by 6–8 kcal mol^{-1} and a larger reduction in these barriers is expected if the selenol is deprotonated either by solvent or the pendant group. Recent modeling studies suggest that the SeCys of GPx is in the selenolate form.[63] The product complexes **P1** are stabilized relative to the PhSeH parent by 6–15 kcal mol^{-1} by the strong Se···N,O interactions between the pendant groups and the weak Se–OH bond (*e.g.*, d(Se–N) = 2.43 in **4a-P1**).

Step 2: *Selenenic acid reduction*. The nucleophilic attack of thiol on the selenenic acid to produce water and the selenenyl sulfide was modeled based upon an S_N2-type pathway. A network of four water molecules arranged in a square cluster was used to bridge the sulfhydryl group to the hydroxyl of the selenenic acid such that the proton exchange occurs between opposite waters of the cluster

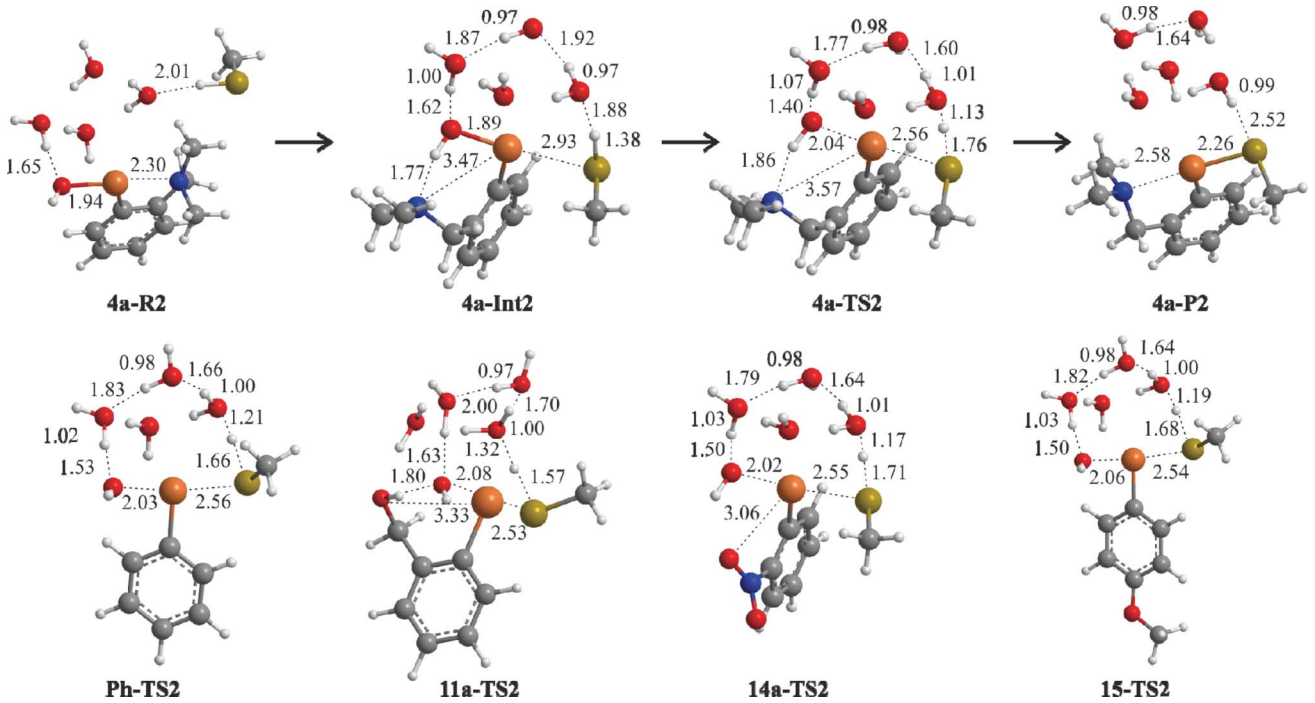

Fig. 4 Selected bond distances for step 2 of the GPx-like mechanism of selenols (selenenic acid reduction). All stationary points are shown for MeSH reduction of **4a-SMe**; TS2 structures are provided for PhSeH,[30] **11a-SMe**, **14a-SMe** and **15-SMe**. All distances are in Ångstroms.

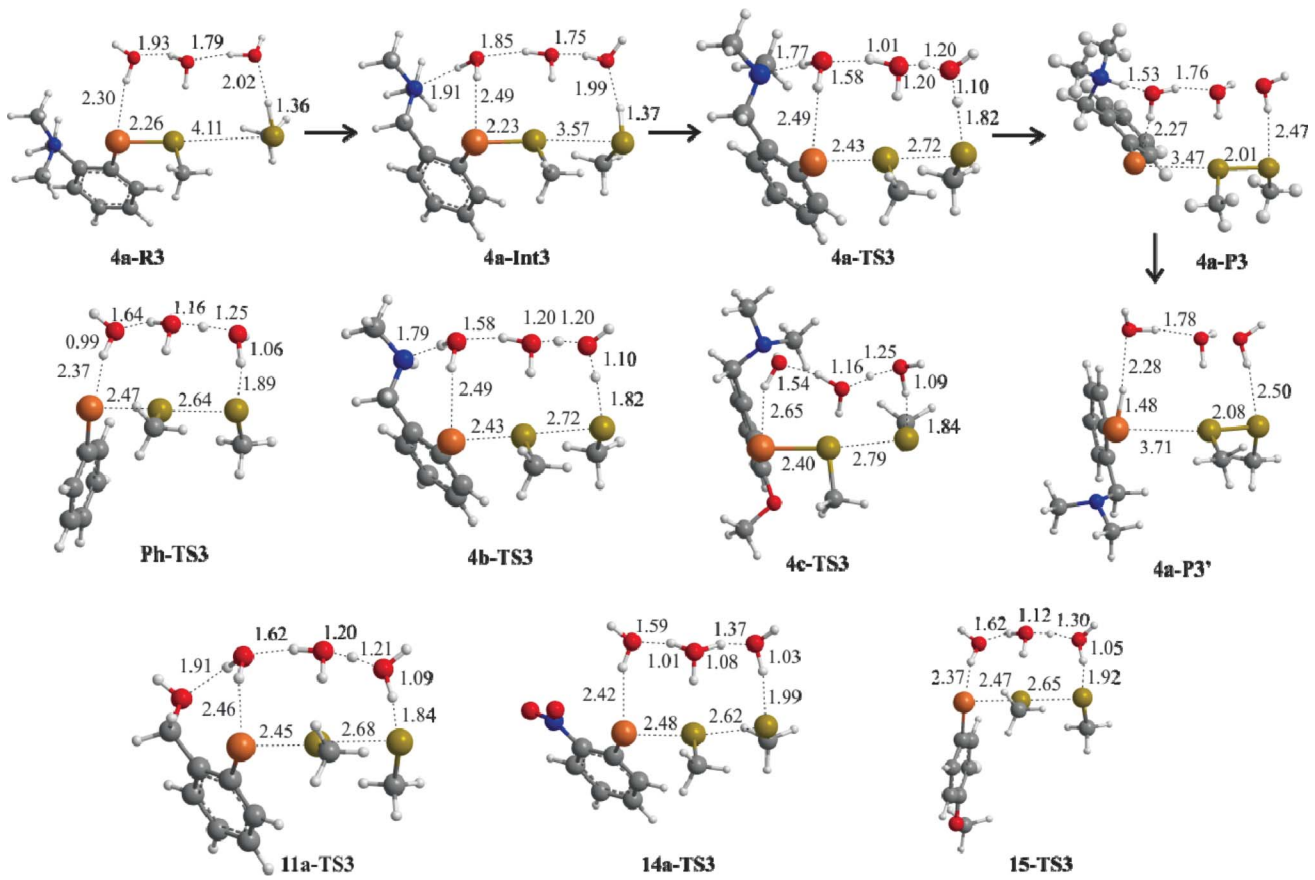

Fig. 5 Selected bond distances for step 3 of the GPx-like mechanism of selenols (selenol regeneration). All stationary points are shown for MeSH reduction of **4a-OH**; TS3 structures are provided for PhSeH,[30] **11a-OH**, **14a-OH** and **15-OH**. All distances are in Ångstroms.

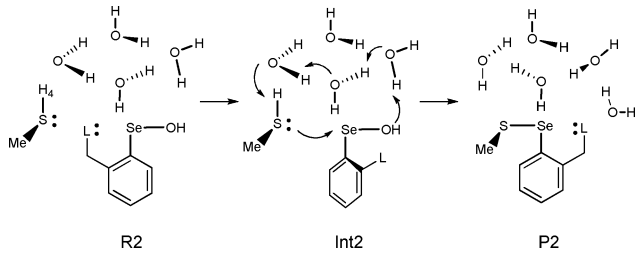

Scheme 3 SAPE network for step 2 of the GPx-like mechanism.

(Scheme 3). In our previous work, this four-water SAPE network was shown to allow a better angle of approach for the back-side attack of the incoming thiol than a smaller two-water network.[30] As a result, a much lower activation barrier was found for R = Ph ($\Delta G+\Delta G_{solv}$ = 6.6 kcal mol^{-1} *versus* 11.1 for the two-water model). Similarly, solvation-corrected activation barriers for reduction of **4a-OH** using a two-water SAPE network was 5 kcal mol^{-1} higher than the four-water model.

For the *ortho*-substituted selenenic acids, coordination of the donor group to the selenium center blocks the approach of the incoming thiol and must be displaced in order for the S_N2-type process to occur. Therefore, the reaction was mapped from intermediate **Int2** in which the incoming thiol is coordinated to selenium and the Se···N,O interaction of **R2** is replaced with the Se···S interaction between the thiol and selenenic acid. The connectivity of the hydrogen bonds of the SAPE network was maintained between **R2** and **Int2** to ensure consistency in the models. In these intermediates, the pendant groups form a strong hydrogen bond to the selenenic acid group with the basic amine of **4a-Int2** (d(N···H) = 1.77 Å, Fig. 5) and a significantly weaker interaction with the -NO_2 group of **14a-Int2** (d(O···H) = 2.03). These hydrogen bonding interactions may decrease the activation barrier by stabilizing the build-up of negative charge on OH. The alcohol group in **11a** may either accept or donate a hydrogen bond to the selenenic acid; the former (denoted **11a-Int2**) is slightly lower in energy and leads to a lower transition state **11a-TS2**. As the thiol is a poor donor for the selenenic acid relative to the pendant groups, the intermediate species **Int2** are higher in energy than the reactant complex (Table 2). Transition states were not determined for the displacement, but are expected to be higher for bulky donor groups or aromatically-stabilized Se···N,O interactions. The relative free energies of **R2** and **Int2** (ΔG_{int}) are roughly consistent with the strength of the interaction of the donor group with the selenenic acid group (Table 2). Displacement of the nitro group in **14a-OH** requires the most energy ($\Delta G_{int}+\Delta G_{solv}$ = 14.9 kcal mol^{-1}) in order to overcome aromatic stabilization. The Se···N,O interactions in **4a-OH** and **11a-OH** are more easily displaced by MeSH, and the uncorrected values of ΔG_{int} (8.8 and 4.7 kcal mol^{-1}, respectively) correlate well with $\Delta E_{d\rightarrow a}$ for the isolated selenenic acids. Corrections for bulk solvation effects respectively stabilize and destabilize **4a-Int2** and **11a-Int2**, but this result may be attributed to the limitations of solvation methods that do not account for solute–solvent hydrogen bonding.

The displacement of the pendant groups increases the overall activation barrier relative to PhSeOH with the lowest barrier found for **11a-TS2** ($\Delta G^{\ddagger}+\Delta G_{solv}$ = 10.5 *vs.* 6.6 kcal mol^{-1}). The **4a-TS2** and **14a-TS2** have higher activation barriers (15.2 and 19.7 kcal mol^{-1}, respectively) given the strong Se···N,O interactions for **4a-OH** and **14a-OH** (see Table 2). Calculated from the intermediates, **11a-TS2** is only 1 kcal mol^{-1} higher than **11a-Int2** where the accumulation of negative charge on O_A is stabilized by a hydrogen bonding interaction between the leaving group to the pendant alcohol (Fig. 4). However, for **4a**, the activation barrier in comparison to **Int2** is higher relative to PhSeOH. In this case, the pendant group contributes the donor atom to the intramolecular hydrogen bond which reduces the partial charge of the proton and strengthens the Se–O bond (Fig. 4). Even with the increase in $\Delta G^{\ddagger}+\Delta G_{solv}$, step 2 remains the lowest barrier for the GPx-like cycle. These higher activation barriers are consistent with the use of internal coordination to stabilize selenenic acids and other divalent reducible RSeX compounds for isolation and the requirement of acid catalysis for the reduction of **14a**-OH through protonation of the leaving group.[64] Kinetics studies of the related nucleophilic substitution reactions of **14a-Br** show a decrease in the reaction rate relative to PhSeBr of $>10^6$.[65]

Step 3: *Selenol regeneration*. The last step of the GPx cycle in which the selenol is regenerated was modeled as an nucleophilic attack on the sulfur center of the selenenyl sulfide with a three water network to facilitate proton exchange (Scheme 4). Mugesh has shown that Se···N,O interactions increase the partial negative charge on the sulfur center (q_S) of the –SeS– group which leads to a preference for attack at the more electrophilic selenium center for a net thiol exchange reaction.[17] In order for step 3 to proceed in the presence of Se···N,O interactions, the donation of electron density to the σ* orbital must be broken to relieve the partial hypervalency and reduce q_S. Therefore, step 3 will be most favored for *ortho*-substituted arylselenols with weak, labile donor–acceptor interactions. Because aromatic stabilization significantly strengthens the Se···N,O interaction, selenols and diselenides containing unsaturated donor groups, like **5** and the ebselen derivative **10a**, are poor or inactive GPx-like mimics.

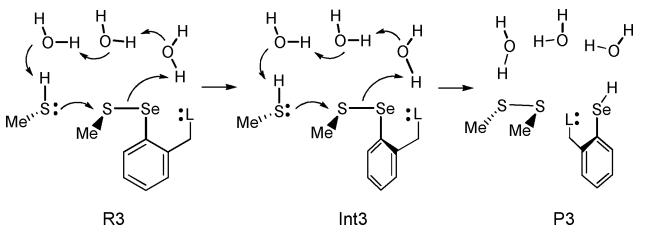

Scheme 4 SAPE network for step 3 of the GPx-like mechanism.

The reactant complex **R3** consists of an S···S interaction between the thiol and the sulfur center of the –SeS– group. The thiol proton is connected to the selenium center by a three-water SAPE network. Similar to step 2, the pendant group donating to Se must be displaced in order to find the transition state. In **Int3**, the donor group forms a hydrogen-bonding interaction with the proton of the terminal water not involved in proton transfer. An alternate arrangement in which the pendant group is moved toward the Me group of SeS is less stable and produces a slightly larger activation barrier. Displacement of the donor group from selenium coordination depends upon the relative strength of the Se···N,O interaction and the hydrogen bond to the water. Generally, the Se···N,O interaction is stronger and **Int3** lies several kcal mol^{-1} above **R3** (Table 3). The one exception is the *ortho* alcohol **11a-Int3** for which the relative enthalpy is

negative and the ΔG_{int} (uncorrected for solvation effects) is slightly positive. These results are attributed to comparable strengths of the Se–O interaction in **11a-R3** and the hydrogen bond in **11a-Int3**. Consistent with Mugesh's hypothesis of the negative charge on S, the APT charges on the –SeS– sulfur center changes dramatically from **R3** to **Int3**. For example, for **4a-R3**, the sulfur charge decreases from –0.29e to +0.04e in **4a-Int3**. In addition to the change in charges, d(S···S) decreases by 0.55 Å further indicating the increase in electrophilicity of the selenenyl sulfide sulfur upon disruption of the Se···N,O interaction. Similar changes in charge and the S···S interaction were calculated for all species.

From **Int3**, the transition states **TS3** (Fig. 5) are characterized as the formation of the S–S bond concurrent with proton transfer to the SAPE network. Consistent with the stabilizing effect of the Se···N,O interaction, each of the activation barriers calculated from **R3** are greater than the parent PhSeSMe (Table 3) although most barriers calculated relative to **Int3** are similar to or lower in energy than for PhSeSMe. In addition to **4a**, **11a**, **14a**, and **15**, we have calculated activation barriers for reduction of **4b-SMe** and **4c-SMe** based upon recent work by Mugesh.[56,62,59] Ortho-substitution of benzylic amines were shown to be more robust GPx mimics than their amide counterparts.[59] *tert*-Amines such as **4a** have long been examined as GPx mimics. These compounds readily react with thiol to generate selenol and selenenyl sulfide intermediates which scavenge peroxide by GPx-like mechanisms. Transition state **4a-TS3** (Fig. 5) occurs earlier along this coordinate relative to **Ph-TS3** with a longer S–S bond distance (2.72 Å) and a shorter S–H bond for the proton being transferred to the network. The SAPE activation barrier is ~5 kcal mol^{-1} higher than the parent reaction, primarily due to stabilization of the Se–S bond by the Se···N interaction. The barrier calculated from **4a-Int3** where the amine interacts with the SAPE network rather than Se is 3 kcal mol^{-1} lower than the parent because the hydrogen bond stabilizes the proton transfer from the thiol to the SAPE network. Due to the basicity of the amine, the proton is transferred to the amine rather than the selenium producing a zwitterionic selenolate **4a-P3**. The rearranged conformation with the amine donating to the Se–H bond of the selenol (**4a-P3′**, Fig. 5) is lower in enthalpy, but non-spontaneous (Table 3). The zwitterionic product complex is favored for each amine-substituted selenenyl sulfide in Table 3 with the selenol product preferred by the less basic oxygen donors.

Mugesh has shown that the analogous *sec* amines such as **4b** are substantially more active than their *tert* amine counterparts because their selenenyl sulfides do not react *via* thiol exchange. These results are qualitatively consistent with our models of step 3 in which **4b-SMe** has a slightly lower activation barrier to selenol regeneration than **4a-SMe** (Table 3) with a surprisingly similar structure for TS3 (Fig. 5). However, our NBO calculations of **4a-SMe** and **4b-SMe** suggest that the donor–acceptor interaction is actually stronger in the *sec*-amine (13.3 kcal mol^{-1}) with comparable NPA sulfur charges between the amines (–0.101e and –0.102e, resp.). However, the higher proton affinity of the *sec*-amines results in a stronger hydrogen bonding interaction with the SAPE network in **4b-Int3** which in turn lowers the overall barrier for **4b-TS3**.

Mugesh also showed that the activity of *tert*-amines can be improved by substituting a methoxy group at the 6 position.[56] Steric interference prevents the most favorable conformation of the Se···N,O interaction, a linear arrangement of the Se–S bond and the donor atom, and, thus, increases the electrophilicity of the selenenyl sulfide sulfur. DFT studies of **4c-SPh** showed that the N–Se–S angles for the 6-MeO derivatives were 10–20° smaller than the parent compounds and that the Se–N bond distance increased by ~0.2 Å relative to **4a-SPh**.[56] Steric interference also reduced the NBO $\Delta E_{d\rightarrow a}$ value for **4c-SPh** (5.8 *versus* 15.2 kcal mol^{-1}) and produced a more positive partial charge at the –SeS– sulfur (0.067e *versus* 0.023e).[56] Mugesh's kinetics study showed an improvement in the rates of peroxide scavenging that was attributed these weaker Se···N,O interactions to the extent that the **4c** is a highly effective GPx mimic. Consistent with these experimental observations, the activation barrier for **4c-TS3** is 6 kcal mol^{-1} lower than that for **4a-TS3** and occurs earlier along the S–S bond formation coordinate (Fig. 5: d(S–S) = 2.79 *versus* 2.72 Å).

High-energy transition states are found for those compounds for which aromatic stabilization must be overcome in order to form **Int3**. The Se···O interactions for both **14a-SMe** and the ebselen derivative **10a-SMe**[66] are strengthened by the additional stabilization due to contributions from the resonance structures shown in eqn (4). As a result, the energy required to displace the donor groups from the selenenyl sulfides is higher than for most other donor groups. Additionally, TS3 is high-energy (26.7 (**14a-TS3**) and 30.8 (**10a-TS3**)[66] kcal mol^{-1}) and generally occurs later along the reaction coordinate (Fig. 5). Disruption of aromatic stabilization by using a *tert*-amide (*i.e.*, **10c**) in which steric effects between the amide R groups and the phenyl ring prevent the formation of a planar ring conformation significantly increases the GPx-like activity of amide-based diselenides.[62]

For the remaining selenenyl sulfides without unsaturated donor groups, the reduction of **11a-SMe** has the second lowest overall activation barrier (22.5 kcal mol^{-1}). Wirth showed that the activity for catalytic scavenging of H_2O_2 or *t*BuOOH using alcohol (**11c**) and ether (**11b**) diselenides was lower than that for the *para*-methoxy derivative **15** (*e.g.* in H_2O_2: 26.6 (**11c**) *versus* 30.2 (**15**) nmol NADPH/min).[15] The lower GPx-like activity for the *ortho*-substituted compounds is consistent with the higher barrier for **11a-TS3** relative to **15-TS3**(Table 3). Experimentally, the ether **11d** has approximately half the activity of **11c** even though the NBO donor acceptor energies are similar for **11a-SMe** and **11b-SMe** ($\Delta E_{d\rightarrow a}$ (DFT(mPW1PW91)/BSI) = 5.0 *versus* 4.5 kcal mol^{-1}). Later studies by Tripathi *et al.*[8] showed that **11a** is more active than **15** under similar conditions consistent with the aromatically-stabilized Se···O interaction in **13-SMe** (9.2 kcal mol^{-1}). Assuming that step 3 is the rate determining step, the greater ability of the -OH group to hydrogen bond with the surrounding solvent as reflected in $\Delta H_{R3\rightarrow Int3}$ for **11a** may favor displacement of the Se···O interaction for alcohol donors to increase the overall activity.

Conclusions

The strength of the Se···N,O interaction for a given Se–X acceptor is primarily due to the strength of the Lewis base donor. Secondary effects from steric factors and aromatic stabilization weaken and strengthen the interaction, respectively. The effect of these Se···N,O interactions on the GPx-like mechanism (Scheme 1) has been demonstrated using DFT-SAPE models of several substituted selenols: (a) the pendant group lowers the barrier for step 1 (selenol oxidation), but only when corrected

for bulk solvation effects; (b) *ortho* substituents block the attack of the thiol to slightly increase the activation barrier to reduction of the selenenic acid (step 2); and (c) weak Se···N,O interactions with the selenenyl sulfide of step 3 are preferred as they make it easier for the donor group to be displaced from the selenium and, thus, reduce the partial charge of the selenenyl sulfide sulfur center. These mechanistic insights should enhance the design of effective GPx mimic through an understanding of the role played by the donor groups at each stage of the reaction.

Steric effects of bulky R groups have not been included in the SAPE mechanisms, but have been shown to have important effects on GPx-like activity. For example, the half-life of diselenide GPx-like activity decreases with bulkier R groups (Me < Et < nPr < iPr).[59,62] This dependence is of interest in light of the importance of Se···N,O interactions that hold these groups in close proximity to the selenium center. These groups probably do not significantly impede the approach of the thiol to the sulfur end of the selenenyl sulfide in step 3, the presumed rate-determining step, but they may decrease the rate of competition by thiol exchange. Interestingly, the half-life also decreases with bulkier oxidants as shown by Wirth, Mugesh and Iwaoka (H_2O_2 < *t*BuOOH < CumOOH).[15,56,59,62,67] These results suggest that the overall GPx-like may be related to steric factors that limit selenol oxidation. Note that the uncorrected step 1 activation enthalpies (Table 1) are comparable to those for step 3 (Table 3). Bulky groups on the oxidant and pendant group reduce the probability of successful reactive collisions to lower the rate constant. If the rate constants for step 1 and 3 are similar, then the kinetics of the reaction cannot be described in the simplified terms of a single rate determining step. Note that for *sec*-amides such as **10a** in which the activation barrier for step 3 is high and clearly a rate determining step, there is no dependence upon either the amide or the oxidant R group and saturation kinetics are not observed.

Considering that the selenenyl sulfide appears to be a 'terminal' intermediate due to the higher barrier for step 3, alternate mechanisms have been proposed to understand how these molecules act catalytically. For example, over-oxidation to the seleninic acid[19] or formation of a cyclic seleninate in the case of an alcohol-based diselenide like **11a**[8] have been suggested as possible intermediates. Also, if selenenyl sulfides are as unreactive as they appear, diselenides may be ineffective choices as GPx mimics because half of their selenium equivalents produced by reaction with thiols are trapped as selenenyl sulfides. Clearly, additional questions remain about the catalytic pathways available to these molecules. These and other alternate mechanisms are currently being explored using DFT-SAPE modeling which has been shown to be an effective method for modeling reaction mechanisms of aqueous-phase reactions.

Notes and references

1 G. Mugesh, W.-W. du Mont and H. Sies, *Chem. Rev.*, 2001, **101**, 2125–2180.
2 G. Mugesh and H. B. Singh, *Chem. Soc. Rev.*, 2000, **29**, 347–357.
3 H. Tapiero, D. M. Townsend and K. D. Tew, *Biomed. Pharmacother.*, 2003, **57**, 134–144.
4 H. E. Ganther and J. R. Lawrence, *Tetrahedron*, 1997, **53**, 12299–12310.
5 A. J. Mukherjee, S. S. Zade, H. B. Singh and R. B. Sunoj, *Chem. Rev.*, 2010, **110**, 4357–4416.
6 T. Schewe, *Gen. Pharmacol.*, 1995, **26**, 1153–169.
7 P. A. Lapchak and J. A. Zivin, *Stroke*, 2003, **34**, 2013–2018.
8 S. K. Tripathi, U. Patel, D. Roy, R. B. Sunoj, H. B. Singh, G. Wolmershäuser and R. J. Butcher, *J. Org. Chem.*, 2005, **70**, 9237–9247.
9 T. G. Back and Z. Moussa, *J. Am. Chem. Soc.*, 2002, **124**, 12104–12105.
10 T. G. Back and Z. Moussa, *J. Am. Chem. Soc.*, 2003, **125**, 13455–13460.
11 T. G. Back, Z. Moussa and M. Parvez, *Angew. Chem., Int. Ed.*, 2004, **43**, 1268–1270.
12 T. G. Back, D. Kuzma and M. Parvez, *J. Org. Chem.*, 2005, **70**, 9230–9236.
13 J. A. Ritchey, B. M. Davis, P. A. Pleban and C. A. Bayse, *Org. Biomol. Chem.*, 2005, **3**, 4337–4342.
14 G. Mugesh and W.-W. du Mont, *Chem.–Eur. J.*, 2001, **7**, 1365–1370.
15 T. Wirth, *Molecules*, 1998, **3**, 164–166.
16 V. P. Singh, H. B. Singh and R. J. Butcher, *Eur. J. Inorg. Chem.*, 2010, 637–647.
17 B. K. Sarma and G. Mugesh, *J. Am. Chem. Soc.*, 2005, **127**, 11477–11485.
18 K. Srivastava, T. Chakraborty, H. B. Singh, U. P. Singh and R. J. Butcher, *Dalton Trans.*, 2010, **39**, 10137–10141.
19 K. P. Bhabak and G. Mugesh, *Acc. Chem. Res.*, 2010, **43**, 1408–1419.
20 O. Epp, R. Ladenstein and A. Wendel, *Eur. J. Biochem.*, 1983, **133**, 51.
21 C. Jacob, W. Maret and B. L. Vallee, *Proc. Natl. Acad. Sci. U. S. A.*, 1999, **96**, 1910–1914.
22 H. Blessing, S. Kraus, P. Heindl, W. Bal and A. Hartwig, *Eur. J. Biochem.*, 2004, **271**, 3190–3199.
23 C. A. Bayse and S. Antony, *Main Group Chem.*, 2007, **6**, 185–200.
24 Z. Benkova, J. Kóňa, G. Gann and W. M. F. Fabian, *Int. J. Quantum Chem.*, 2002, **90**, 555–565.
25 J. K. Pearson and R. J. Boyd, *J. Phys. Chem. A*, 2006, **110**, 8979–8985.
26 J. K. Pearson and R. J. Boyd, *J. Phys. Chem. A*, 2007, **111**, 3152–3160.
27 J. K. Pearson and R. J. Boyd, *J. Phys. Chem. A*, 2008, **112**, 1013–1017.
28 C. A. Bayse and S. Antony, *J. Phys. Chem. A*, 2009, **113**, 5780–5785.
29 C. A. Bayse, *J. Inorg. Biochem.*, 2010, **104**, 1–8.
30 C. A. Bayse, *J. Phys. Chem. A*, 2007, **111**, 9070–9075.
31 C. A. Bayse, *Org. Biomol. Chem.*, 2011, **9**, 4748–4751.
32 B. Kallies and R. Mitzner, *J. Mol. Model.*, 1998, **4**, 183–196.
33 Z. Wu, F. Ban and R. J. Boyd, *J. Am. Chem. Soc.*, 2003, **125**, 6994–7000.
34 A. Lundin, I. Panas and E. Ahlberg, *J. Phys. Chem. A*, 2007, **111**, 9080–9086.
35 R. Prabhakar, T. Vreven, K. Morokuma and D. G. Musaev, *Biochemistry*, 2005, **44**, 11864–11871.
36 G. Mugesh, A. Panda, H. B. Singh and R. J. Butcher, *Chem.–Eur. J.*, 1999, **5**, 1411–1421.
37 S. Kumar, K. Kandasamy, H. B. Singh, G. Wolmershäuser and R. J. Butcher, *Organometallics*, 2004, **23**, 4199–4208.
38 C. Adamo and V. Barone, *J. Chem. Phys.*, 1998, **108**, 664–675.
39 *Gaussian 03, Revision D.01*, Gaussian, Inc, Wallingford, CT, 2004.
40 M. M. Hurley, L. F. Pacios, P. A. Christiansen, R. B. Ross and W. C. Ermler, *J. Chem. Phys.*, 1986, **84**, 6840–6853.
41 W. R. Wadt and P. J. Hay, *J. Chem. Phys.*, 1985, **82**, 284–298.
42 T. H. Dunning, *J. Chem. Phys.*, 1971, **55**, 716–723.
43 T. H. Dunning, *J. Chem. Phys.*, 1970, **53**, 2823–2833.
44 J. Tomasi, B. Mennucci and R. Cammi, *Chem. Rev.*, 2005, **105**, 2999–3094.
45 A. Bondi, *J. Phys. Chem.*, 1964, **68**, 441–451.
46 D. H. R. Barton, M. B. Hall, Z. Lin, S. I. Parekh and J. Reibenspies, *J. Am. Chem. Soc.*, 1993, **115**, 5056–5059.
47 C. A. Bayse, R. A. Baker and K. N. Ortwine, *Inorg. Chim. Acta*, 2005, **358**, 3849–3854.
48 A. E. Reed, L. A. Curtiss and F. Weinhold, *Chem. Rev.*, 1988, **88**, 899–926.
49 M. Iwaoka and S. Tomoda, *J. Am. Chem. Soc.*, 1994, **116**, 2557–2561.
50 M. Iwaoka and S. Tomoda, *J. Org. Chem.*, 1995, **60**, 5299–5302.
51 M. Iwaoka and S. Tomoda, *J. Am. Chem. Soc.*, 1996, **118**, 8077–8084.
52 M. Iwaoka, H. Komatsu, T. Katsuda and S. Tomoda, *J. Am. Chem. Soc.*, 2004, **126**, 5309–5317.
53 M. Iwaoka and S. Tomoda, *Phosphorus, Sulfur Silicon Relat. Elem.*, 2005, **180**, 755.
54 M. Iwaoka, H. Komatsu, T. Katsuda and S. Tomoda, *J. Am. Chem. Soc.*, 2002, **124**, 1902–1909.
55 M. Iwaoka, T. Katsuda, H. Komatsu and S. Tomoda, *J. Org. Chem.*, 2005, **70**, 321–327.
56 K. P. Bhabak and G. Mugesh, *Chem.–Eur. J.*, 2008, **14**, 8640–8651.
57 C. A. Bayse and B. D. Allison, *J. Mol. Model.*, 2006, **13**, 47–53.
58 C. A. Bayse and S. Antony, *Molecules*, 2009, **14**, 3229–3236.
59 K. P. Bhabak and G. Mugesh, *Chem.–Eur. J.*, 2009, **15**, 9846–9854.

60 R. M. Minyaev and V. I. Minkin, *Can. J. Chem.*, 1998, **76**, 776–788.
61 R. M. Minyaev and V. I. Minkin, *Mendeleev Commun.*, 2000, **10**, 173–174.
62 K. P. Bhabak and G. Mugesh, *Chem.–Asian J.*, 2009, **4**, 974–983.
63 S. T. Ali, S. Jahangir, S. Karamat, W. M. F. Fabian, K. Nawara and J. Kóna, *J. Chem. Theory Comput.*, 2010, **6**, 1670–1681.
64 J. L. Kice, F. McAfee and H. Slebocka-Tilk, *J. Org. Chem.*, 1984, **49**, 3106–3114.
65 T. Austad, *Acta Chem. Scand., Ser. A*, 1975, **29**, 895–906.
66 S. Antony and C. A. Bayse, *Inorg. Chem*, 2011, DOI: 10.1021/ic201603v.
67 B. G. Singh, P. P. Bag, F. Kumakura, M. Iwaoka and K. I. Priyadarsini, *Bull. Chem. Soc. Jpn.*, 2010, **83**, 703–708.